International Journal of
Advances in Scientific Research and Engineering (ijasre)

E-ISSN : 2454-8006

DOI: 10.31695/IJASRE.2020.33939

Volume 6, Issue 12
December - 2020

Influence of P^H, Immersion Time and Inhibitor Concentration on the Corrosion Inhibition Characteristic of *Citrullus Lanatus* Extract on A36 Carbon Steel in A CO_2 Saline Solution

Afoegba Clement . S[1]., Agbonkhese, Kingsley A[2]., Onobrenufe, Oghenero[3]

[1]Department of Welding Engineering and Offshore technology, Petroleum Training Institute (PTI), Efurun, Delta State, Nigeria

[2]Department of Mechanical Engineering Technology, National Institute of Construction Technology and Management (NICTM), Uromi, Edo State, Nigeria

[3]Department of Atomic Absorption Spectrophotometer, Thermosteel Nigeria Limited (Analytical/ Environmental Laboratory), Enerhen Road, Efurun, Delta State, Nigeria

ABSTRACT

The use of Watermelon Seed Extract was employed to monitor the corrosion process of A36 Carbon Steel using varying pH (3.15-8.0), Immersion Time (24hrs-120hrs) and Inhibitor Concentration (50-200ppm). A 3.5wt% Sodium Chloride solution was prepared by dissolving 3.5g of NaCl in deionised water. Carbon (IV) oxide gas was bubbled onto the saline solution with the corresponding Ph measured and recorded using a calibrated Ph Meter (HANNA). Varying concentration (50-200ppm) of the Inhibitor was introduced into the Solution. A36 Carbon Steel Coupon was immersed into the CO_2 Saline solution of varying PH. Weight Loss and Inhibition Efficiency was employed to test the investigation. Scanning Electron Microscope Analysis on the surface morphology of the Carbon Steel Coupon with and without the Inhibitor was carried out to corroborate the findings.

Key Words: Immersion, Inhibitors, Corrosion, Citrullus Lanatus, Characteristics.

1.0 INTRODUCTION

Carbon Steel is recognised as a frequently used material by Industries for construction activities (Fayomi et al., 2019; Rivera-Grau et al., 2012). These Carbon steels often times are seriously faced with incidence of high corrosion rate in an Environment that is mostly Saline which also contains a very high concentration of Carbon (IV) Oxide (Asadi et al., 2015) . Due to Carbon (IV) Oxide presence, there is often a resulting sweet corrosion that arises as a result of Carbonic acid and Hydrogen Carbonate formation (El-Lateef et al., 2012). The presence of Carbonic acid acutely increases the rate of corrosion (Alan, et al., 2020). Although, studies have shown that Corrosion rate is strongly dependent on a number of factors namely, Temperature, Flow, pH, pressure, the chemistry of the solution etc (Obot et al., 2019).

Due to the risks associated with Corrosion, several techniques such as cathodic protection, use of corrosion resistance materials, Addition of corrosion Inhibitors etc have been developed over time (Yabuki, et al., 2018: Lyon, et al., 2017: Salman, et al., 2018: Odewunmi, et al., 2015) . Among the different Techniques, addition of corrosion Inhibitors on the metal surface has been the most widely considered technique (Go et al., 2019; Qian et al., 2009). Corrosion Inhibitors are remarkably used in both flow and closed systems. It should be noted that among the Corrosion Inhibitors, the Inhibitors that are compatible with the environment are described as green Inhibitors or Eco-friendly

Inhibitors (Cen et al., 2019). They have great ability in inhibiting the corrosion on metal surface owing to their non-toxic nature and biodegradability. Though, the ingredient responsible for the adsorption of the green Inhibitors onto the Metal surface varies from different Plant species to the other (Obot et al., 2019; Zhang et al., 2016).

The Hydrogen ion concentration in a solution can be regarded as a very significant variable in a Carbon (IV) Oxide induced corrosion (Anbari, et al., 2013) (Durowaye et al., 2014). Historically, it has been found that computational and experimental studies have demonstrated that any change in the pH of the solution has a notable impact on the rate of corrosion (Durowaye et al., 2014) and this effect can either be in a direct or in an indirect process (Peng and Zeng, 2015). Directly, it has been observed that an increase in pH causes a decrease in the rate of Carbon (IV) Oxide corrosion due to the limited concentration of Hydrogen ion, which invariably depicts less of the cathodic reaction and a resulting lesser corrosion (Palumbo et al., 2019) . In addition, experiments conducted have revealed that when the pH is less than four, mostly with a low partial pressure of Carbon (IV) Oxide , the straight depletion of Hydrogen ions results to an increase in corrosion rate (Durowaye et al., 2014). Furthermore, when the pH range is within four to six, it has been observed that the cathodic reaction is the reduction of Hydrogen $Carbonate_3$ (Yao, et al., 2020). More so, if the pH of the solution is greater than six, varying investigations have revealed that the cathodic reaction is dominant because of the reduction of bicarbonate (Kina and Ponciano, 2013). It can also be infer from previous studies that in an indirect way, an increase in the pH reduces the solubility of Iron carbonate; which in effect, promotes the precipitation of the carbonate layer at a rate which is very fast and consequently, the corrosion rate decreases (Aribo et al., 2017). Chlorides in seawater is capable of destroying the oxide film on the metal surface and forming a complex with the metal ions (Onyeachu et al., 2020), which in turn will produce hydrogen ions during hydrolysis (Nam et al., 2013), and this behaviour causes an increase in the acidity of sea water and further generates local corrosion on the metal surface (Tariq Saeed et al., 2020).
Previous studies have investigated different means of mitigating the growing effect of corrosion (Dehghani et al., 2019; Farhadian et al., 2020; John et al., 2019; Khan et al., 2017; Ramezanzadeh et al., 2019; Singh et al., 2018: Hu, et al., 2016).

Notably,(Oloruntoba et al., 2020) demonstrated that Water corrosion on Metal surface can be controlled with the use of Herbal Extracts of Nigerian origin. More so,(Hynes et al., 2020) demonstrated that Aerveva lanata Flowers is a suitable corrosion inhibitor due to the hydrazide contents that is present in their fatty acid.

Study conducted by (Al-Haj-Ali et al., 2014) on the Inhibition Characteristics of *Citrullus lanatus* on Aluminum in Acids and Saline Water revealed that the *Citrullus lanatus* oil is a satisfactory Corrosion Inhibitor in aqueous solutions.

Among the previous research (Dehgani, et al., 2019: Gerengi, et al., 2016: Muthukrishna, et al., 2019: Kumar, et al.,2011: Alibakhshi, et al., 2018) on the use of Plant Extract as a Corrosion Inhibitor, very little publications have extensively dealt with the effect of varying the pH and Immersion time on the Corrosion Inhibitor of *Citrullus lanatus* Extract of Nigerian origin in a Carbon (IV) Oxide saturated saline solution.

Thus, this study investigated the use of *Citrullus lanatus* in a Carbon (IV) Oxide saturated saline solution with reference to the effect of pH and Immersion time on the resulting Corrosion control on Carbon Steel surface.

2.0 EXPERIMENTAL

2.1 Materials and Solution

Carbon steel Coupons with size about 20 mm x 40 mm x 2 mm was cut out of the steel sheet and the sample was cleaned by wire brushing base on International Standard Organization (ISO) ISO 8504:2000 (E).The coupon sample was pre-treated prior to the experiment by scrubbing the surface with sand paper to smoothen the surface and then cleaned with distilled water, degreased with acetone and sun-dry before the experiment was performed.

DOI: 10.31695/IJASRE.2020.33939

The experiment was performed in 1000ml of de-aerated and pre-CO_2 saturated NaCl solution. The saline solution was prepared using analytical grade NaCl and deionised water. One litre of NaCl solution of about 1.0%w/v concentration was deoxygenated by passing nitrogen gas for 60minutes.The deoxygenated solution was then be pre-saturated by passing the CO_2 at the rate of about four (4) CO_2 gas bubbles per second until the resulting pH of the solution was recorded at pH 8.0, 6.0, 4.0 until a steady pH of 3.15 was obtained at point of CO_2 saturation.

2.2 Equipment

Water bath of Grant JB series model with temperature ranging from 0^oC – 100^oC: was used for maintaining constant Temperature of the corrosive medium.

Soxhlet extractor by Techmel & Techmel USA model with flask capacity of 1000ml was used for the watermelon seed extract

Adams Equipment analytical balance with model number PGW 753i for precision weighing up to 750g maximum and resolution of 1mg: it will be used for weight measurement of both coupon and plants extract.

Rotary Vapour of Model R-210/215 was used for evaporation and condensation of solvent using a rotating evaporating flask under vacuum. It was used to recover ethanol from the extract mixture.

Phenom Pro XScanning Electronic Microscope (Model: Phenom Pro X. Equipped with magnification range of 80 - 100,000x, ≤ 14nm resolution, up to 32mm (Ø) size and 100mm height was used for surface examination of coupon.

2.3 Weight Loss Measurement

Carbon steel coupon of size about 20 x 40 x 2mm was used for the weight loss experiment and was pre-treated prior to the experiment by scrubbing with sand paper up to 600 grit and then cleaned with double distilled water, degreased with acetone and dried. After weighing accurately using digital balance with sensitivity of ±0.01 mg. Coupons were suspended in 100 ml saline test solutions containing 3.5w% NaCl saturated with CO_2 without and with the different concentration of the Water melon seed extract of different concentration ranging from 50g/L to 200g/L

The measurements were performed on a 24 hourly basis. After the elapsed time, the coupons were retrieved at 24 hours interval progressively for 120 hours. The specimen was rinsed with distilled water and in ethanol for 10 minutes in an ultrasonic bath to remove any corrosion products and avoid salt crystallization from the highly saline solution and reweighed. The weight loss, (in grams), was taken as the difference in the weight of the carbon steel coupons before and after immersion in the test solutions. The tests were performed in duplicate to guarantee the reliability of the results, and the mean value of the weight loss was estimated.The measurements were performed at ambient temperature in the reactors.

The effect of Immersion time, Inhibitor concentration and pH of the solution was investigated. The result was compared with the Solution without the Inhibitor.

In all of the experiment, the Corrosion rate was calculated using the relationship below;

$$C_R = \frac{kw}{At\rho} \qquad (2.1)$$

Where;

k is the weight loss constant given as (87.6)

w is the corrosion weight loss of carbon steel (mg),

A is the area of the coupon,

DOI: 10.31695/IJASRE.2020.33939

t is the exposure time (hours), and

ρ is the density of carbon steel

More so, the Inhibition efficiency was computed using the equation below

$$\eta_w = \frac{w_0 - w_i}{w_i} \times 100 \quad (2.2)$$

Where $w_i$and$w_0$are the weight loss value in presence and absence of inhibitor, respectively.

The Weight Loss in each experiment was also determined using given equation

Weight Loss (g) = Initial Weight – Final Weight (2.3)

2.4 Surface Analysis

In order to observe any changes in surface morphologies of the carbon steel specimen after testing, the specimen was immersed in the test media containing the CO_2 saturated saline solution with and without an inhibitor for 7 days, then cleaned with distilled water and acetone, and dried by exposure to air. The surface morphology of the specimen was then analyzed with a scanning electron microscope (SEM) which is a type of electron microscope that produces images of a sample by scanning it with a focused beam of electrons (Chesnokova et al., 2016; Hassan et al., 2016; Tasić et al., 2018)

3.0 RESULTS AND DISCUSSION

3.1 Weight Loss and Inhibition Efficiency

The weight loss and Inhibition Efficiency were tested at different immersion time such as; 24hrs, 48hrs, 72hrs, 96hrs and 120hrs. The pH of the solution was also varied at pH 3.15, pH 4.0, pH 6.0 and pH 8.0. The results shows decreasing weight loss and increasing inhibition efficiency as the inhibition concentration increases from 50mg/l to 200mg/l at a particular time. This can be attributed to the Inhibitor occupying more active sites that can cause corrosion (Espinoza Vázquez et al., 2020). Furthermore, it was observed that as the immersion time increases, the Weight loss increases and the Inhibition efficiency decreases at pH 3.14 to 4.0.Alternatively, it was observed that as the immersion time increases, Weight loss decreases and the inhibitor efficiency increasesat pH 6.0-8.0. Similar observation was also reported by (Mohammed et al., 2020)

Table 3.1: Weight Loss and Inhibitor Efficiency at 24hrs and pH 3.15

Concentration (mg/L)	Weight Loss (g)	Corrosion Rate (mm/hr)	Inhibitor Efficiency (%)
0 (Control)	6.5	0.565	0
50	5×10^{-4}	0.198	95.76
100	2.8×10^{-4}	0.168	90.68
150	2×10^{-3}	0.168	93.22
200	3×10^{-3}	0.214	89.83

DOI: 10.31695/IJASRE.2020.33939

Table 3.2: Weight Loss and Inhibitor Efficiency at 24hrs and pH 4.0

Concentration (mg/L)	Weight Loss (g)	Corrosion Rate (mm/hr)	Inhibitor Efficiency (%)
0 (Control)	4.0	0.565	0
50	1.9×10^{-3}	0.198	76.42
100	1.5×10^{-3}	0.168	94.34
150	3×10^{-3}	0.168	88.68
200	2×10^{-3}	0.214	92.45

Table 3.3: Weight Loss and Inhibitor Efficiency at 24hrs and pH 6.0

Concentration (mg/L)	Weight Loss (g)	Corrosion Rate (mm/hr)	Inhibitor Efficiency (%)
0 (Control)	2.75	0.565	0
50	2.5×10^{-3}	0.198	51.46
100	1.5×10^{-3}	0.168	94.17
150	1.5×10^{-3}	0.168	94.17
200	1.25×10^{-3}	0.214	95.15

Table 3.4: Weight Loss and Inhibitor Efficiency at 24hrs and pH 8.0

Concentration (mg/L)	Weight Loss (g)	Corrosion Rate (mm/hr)	Inhibitor Efficiency (%)
0 (Control)	2.75	0.565	0
50	2.25×10^{-3}	0.198	91.26
100	1.5×10^{-3}	0.168	94.17
150	1.5×10^{-3}	0.168	94.17
200	1.5×10^{-3}	0.214	95.15

Table 3.5: Weight Loss and Inhibitor Efficiency at 120hrs and pH 3.15

Concentration (mg/L)	Weight Loss (g)	Inhibitor Efficiency (%)
0 (Control)	5.7×10^{-3}	0
50	3.06×10^{-4}	94.64
100	1.73×10^{-3}	69.64
150	2.3×10^{-3}	59.8
200	7.14×10^{-4}	87.50

Table 3.6: Weight Loss and Inhibitor Efficiency at 120hrs and pH 4.0

Concentration (mg/L)	Weight Loss (g)	Inhibitor Efficiency (%)
0 (Control)	7.70	0
50	4.34×10^{-3}	43.71
100	3.83	50.33
150	1.02	86.75
200	1.02	86.75

DOI: 10.31695/IJASRE.2020.33939

Table 3.7: Weight Loss and Inhibitor Efficiency at 120hrs and pH 6.0

Concentration (mg/L)	Weight Loss (g)	Inhibitor Efficiency (%)
0 (Control)	5.66	0
50	0.00326	42.34
100	2.35	58.56
150	1.94	65.77
200	1.43	74.77

From Table 3.7, the Inhibitor Efficiency increases from 0 to 74.77% and the weight loss decreased from 5.66g to 1.43g without the inhibitor concentration (Blank) and with the Inhibitor Concentration (200mg/l). At an immersion time of 120hrs. The increased inhibitor efficiency with the inhibitor concentration was due to the availability of the Inhibitor at a longer time (Taheri et al., 2017). Thus, lower concentration of Inhibitor will be used up on time (Verma et al., 2017) and due to the physical adsorption between the Inhibitor molecules and the Metal surface there will be some active sites which will further cause corrosion (Chaouiki et al., 2020). Conversely, at a higher Inhibitor concentration, there will be more Inhibitor molecules that can occupy active sites with time (120hrs)and this will help to reduce the corrosion activity (Asadi et al., 2015).

Table 3.8: Weight Loss and Inhibitor Efficiency at 120hrs and pH 8.0

Concentration (mg/L)	Weight Loss (g)	Inhibitor Efficiency (%)
0 (Control)	0.0118	0
50	0.0077	34.48
100	3,98	66.38
150	1.73	85.34
200	1.43	87.93

Figures (4.19-4.22) represent the effect of immersion time on the Weight Loss. It was observed that as the exposure time increases, the difference in Weight Loss between each time intervals as seen in figures (4.19-4.22) reduces. It was also observed that as the exposure time increases, the weight loss also decreases with increasing Inhibitor Concentration at varying pH. The reason for this is due to the increase in rate of flow of the Inhibitor with exposure time (Zeng, et al., 2016) thus giving room for more surface coverage on the metal surface which in turn minimizes the rate of corrosion of the Carbon Steel (Loto, 2018; Uddin et al., 2018).

It was observed that there was an increase in Weight Loss from 24hrs to 96hrs and a reduction in Weight Loss at 120hrs when the Inhibitor concentration was 0mg/l (Balnk), 50mg/l and 100mg/l while there was a continuous rise in weight loss during these time intervals when the Inhibitor concentration was 100mg/, 150mg/l and 200mg/l. This behaviour can be attributed to the flow of the Inhibitor molecules in occupying all the active sites of the Carbon Steel and also the rate of reaction (Husaini et al., 2018; Lgaz et al., 2017; Oluyori et al., 2020). During 24hrs to 96hrs the Inhibitor molecules were attaching themselves onto the active sites of the Coupon and became stable after 96hrs of Immersion time but due to the slow reaction, the higher Inhibitor volume could not occupy the active sites completely during the investigation period which resulted in the continuous corrosion taking place (Farhadian et al., 2020; Husaini et al., 2018)

DOI: 10.31695/IJASRE.2020.33939

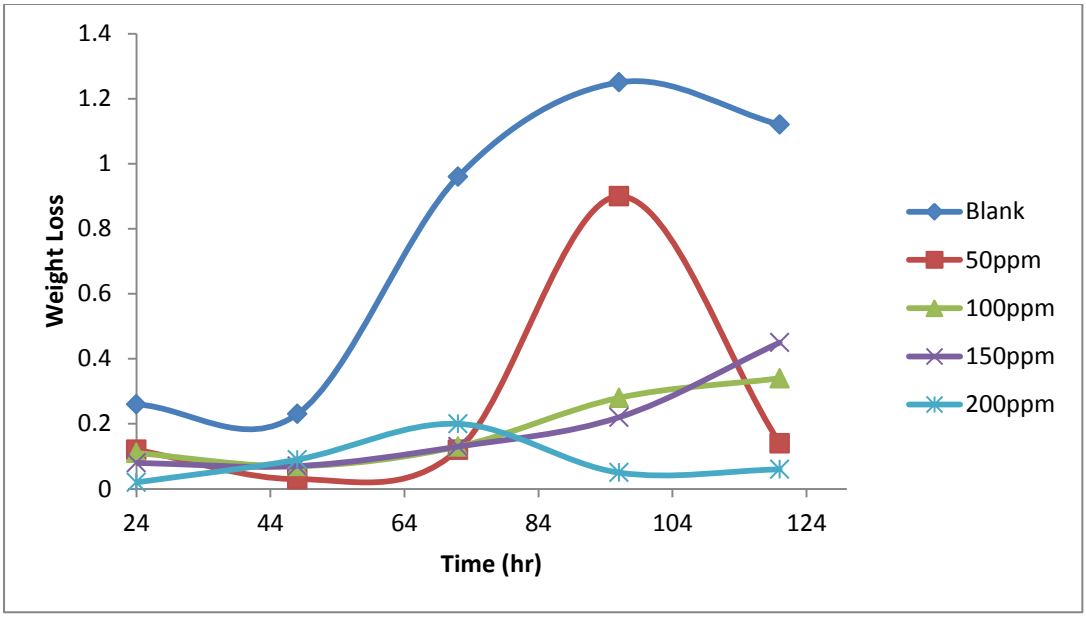

Figure 3.1: Variation of Weight Loss with Time at pH 3.15

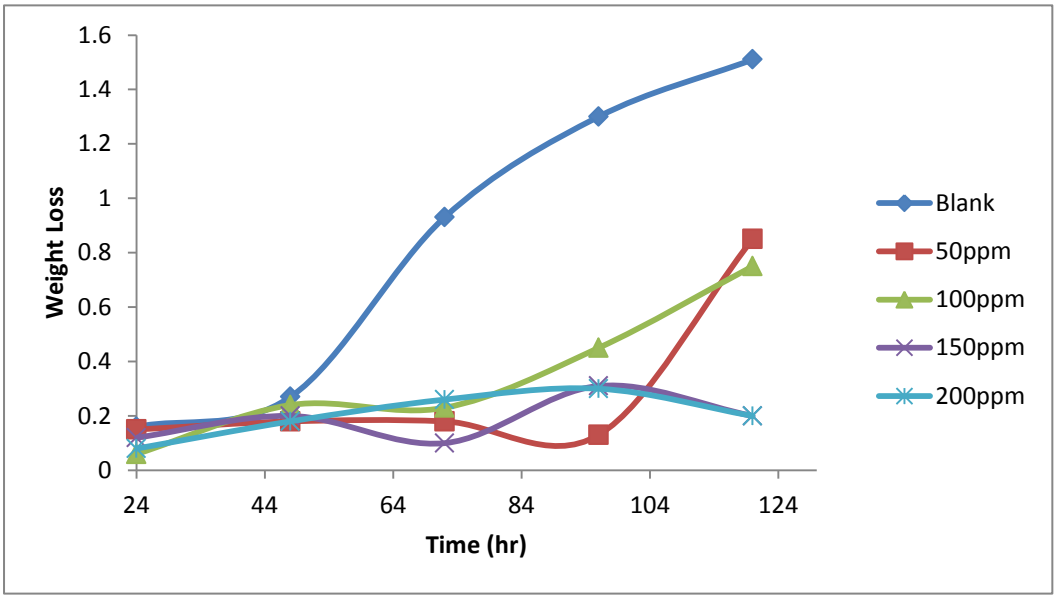

Figure 3.2: Variation of Weight Loss with Time at pH 4.0

DOI: 10.31695/IJASRE.2020.33939

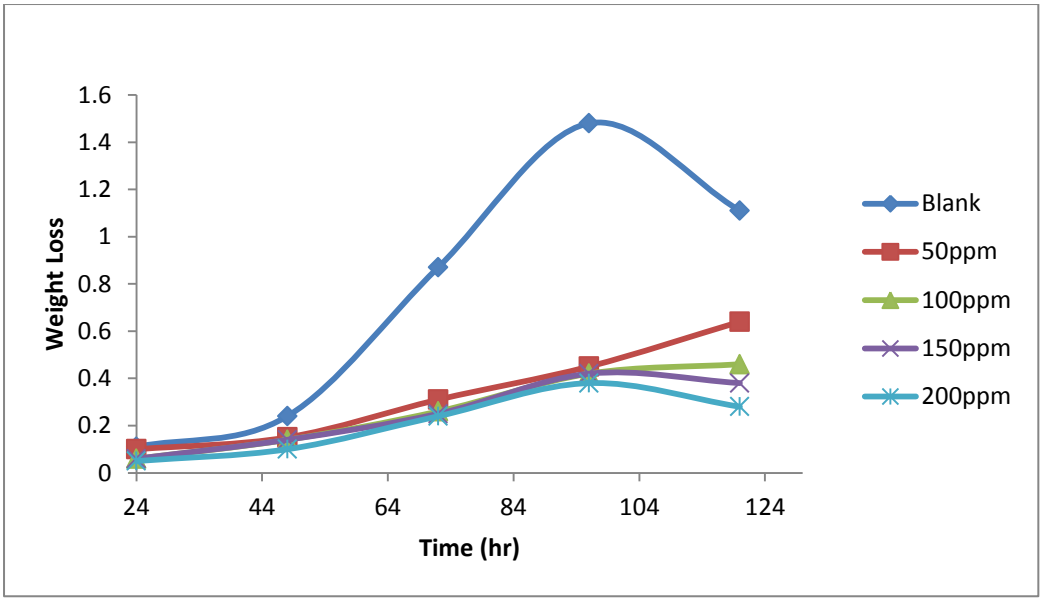

Figure 3.3: Variation of Weight Loss with Time at pH 6.0

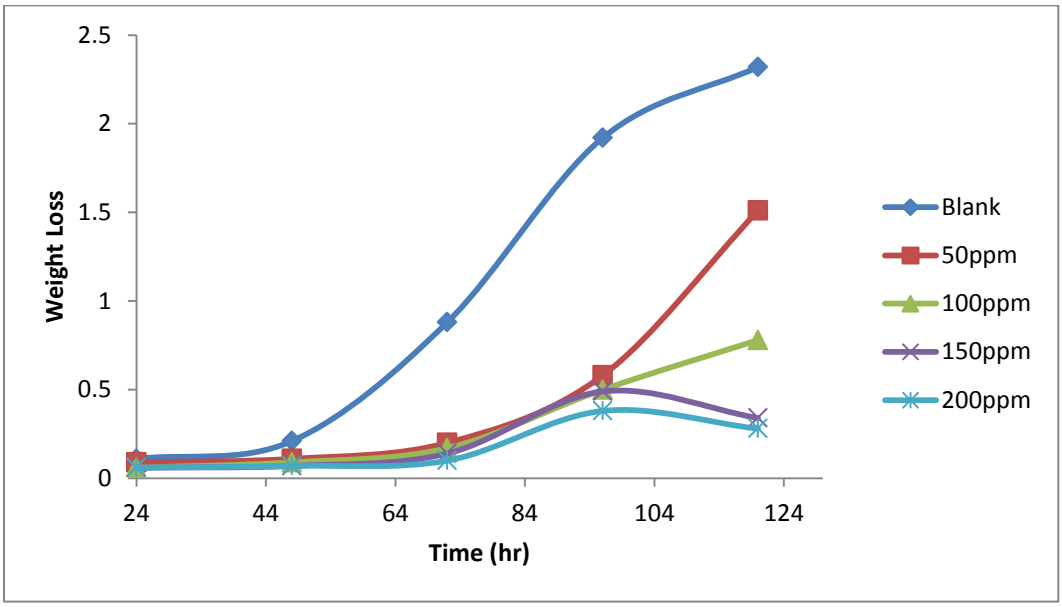

Figure 3.4: Variation of Weight Loss with Time at pH 8.0

DOI: 10.31695/IJASRE.2020.33939

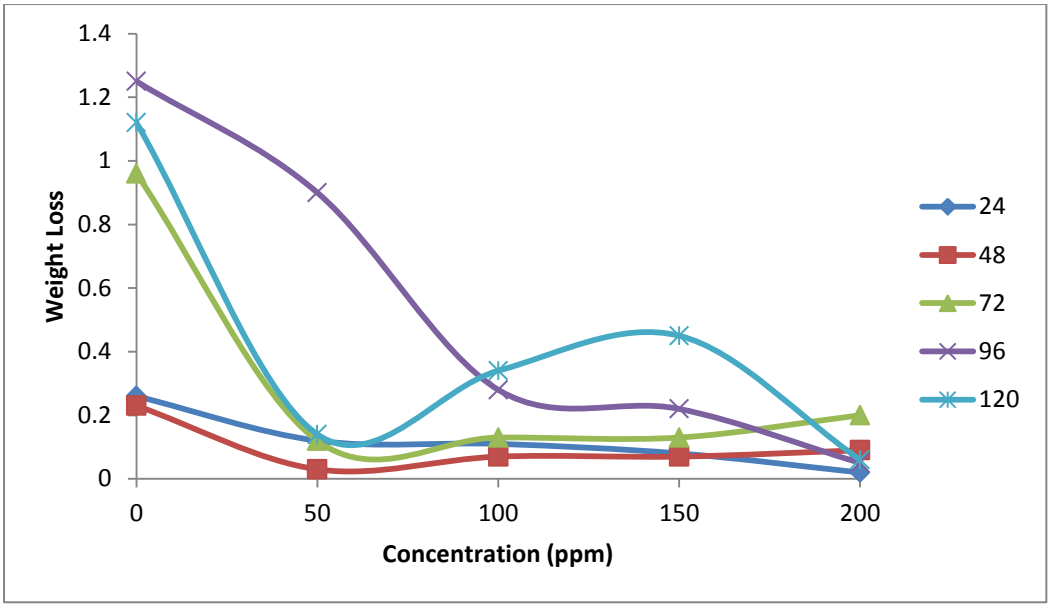

Figure 3.5: Variation of Weight Loss with Concentration at pH 3.15

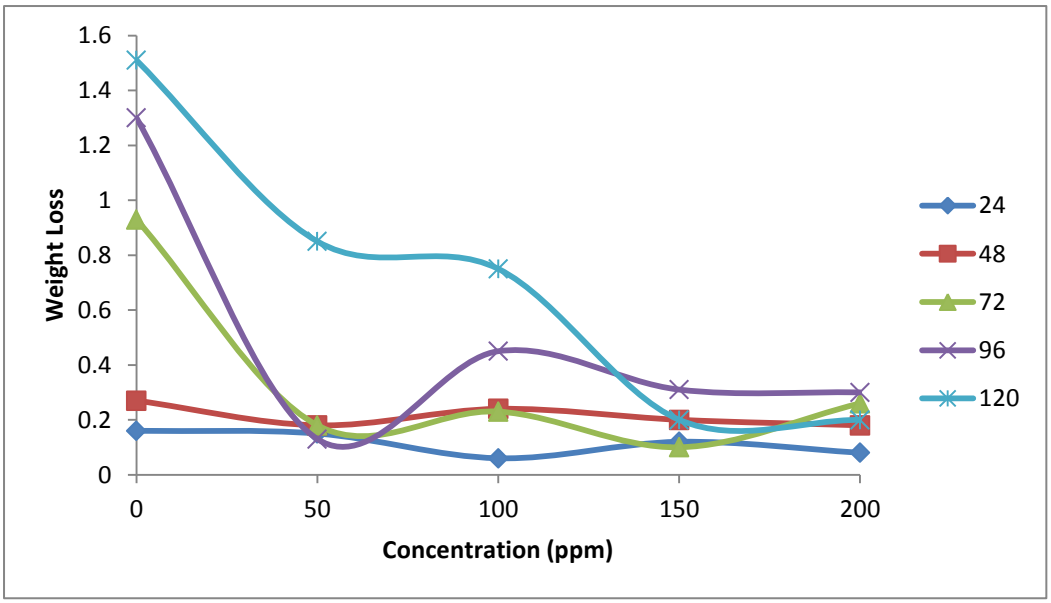

Figure 3.6: Variation of Weight Loss with Concentration at pH 4.0

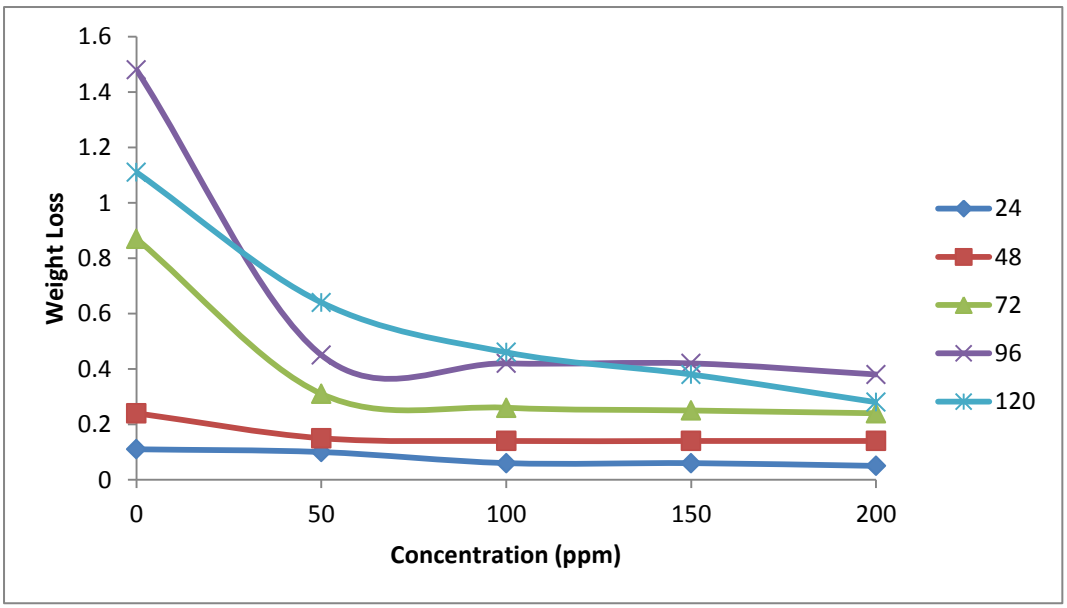

Figure 3.7: Variation of Weight Loss with Concentration at pH 6.0

DOI: 10.31695/IJASRE.2020.33939

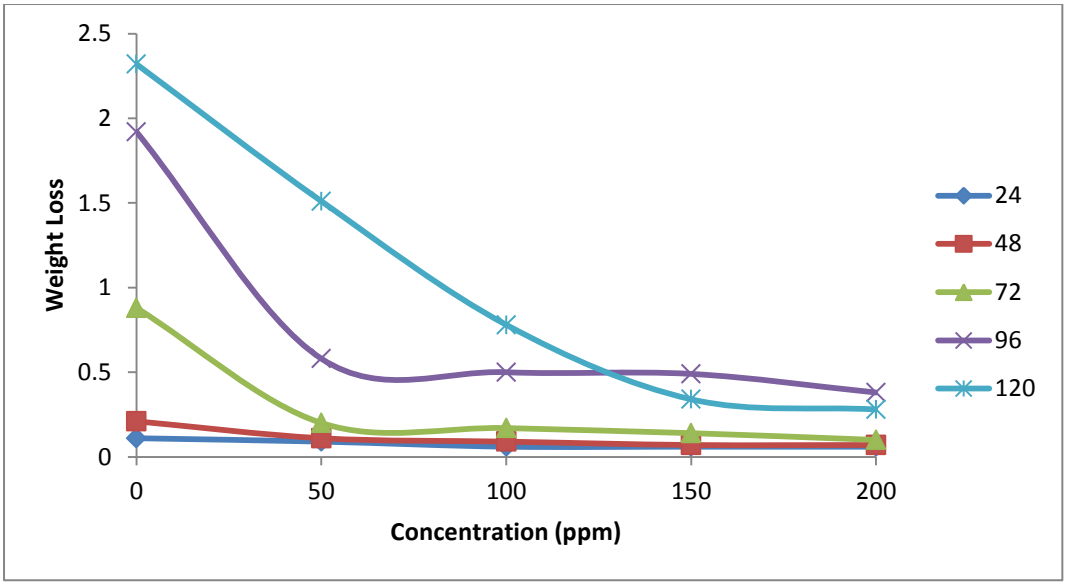

Figure 3.8: Variation of Weight Loss with Concentration at pH 8.0

3.2 Adsorption Isotherm

The Langmuir adsorption isotherm was used to fit the experimental data at different pH (3, 15, 4.0, 6.0 and 8.0).

The Langmuir adsorption isotherm was calculated using the relationship below

$\frac{C}{\emptyset}$= K+C 3.1

Where;

C = The Inhibitor concentration

∅= The degree of surface covered by the inhibitor

K = Adsorption equilibrium constant

Table 3.9: The kinetic data obtained from the Langmuir isothermal plot are shown below;

pH	Slope	Adsorption Constant	Coefficient of determination, R2
3.15	1.1	1.06	0.906
4	1.2	4.2	0.992
6	0.9	0.0061	0.693
8	1.1	1.6	0.997

From Table 3.9, the slope of the adsorption isotherm for the different pH was close to unity with a little variance and this suggests that inhibitor occupies individual active sites of the A36 Carbon Steel (Ardakani et al., 2020). It was observed that the Inhibitor was strongly adsorbed on the Carbon Steel Coupon at pH 8.0 the highest adsorption constant (1.6) was recorded in this study as observed in Table 3.9. Investigation reported by (Palumbo et al., 2019) corroborates this study.

3.3 Gibbs Free Energy

The Gibbs free energy was determined using the relationship below

G= -RTIn55kads 3.2

DOI: 10.31695/IJASRE.2020.33939

Where;

K_{ads} =Adsorption constant

R =The universal gas constant (8.314 J/mol)

T = Temperature

Table 3.10: The Gibbs free energy obtained at various pH is as shown below

pH Level	Gibbs Free Energy (KJ/Mol)
3.15	-1.11
4	-1.16
6	-0.87
8	-1.14

The negative values of the Gibbs free energy observed indicates that the Inhibitor action on the surface of the Carbon steel causes the reaction to be spontaneous (Chakravarthy and Mohana, 2014).

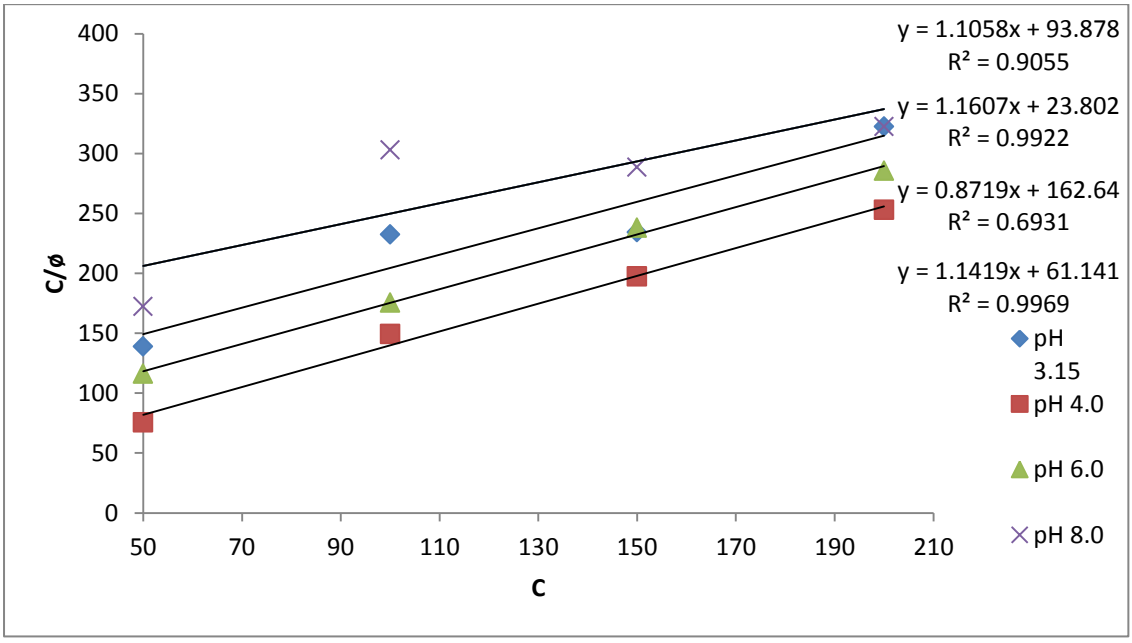

Figure 3.9: Langmuir adsoption Isotherm plot

3.4 Scanning Electron Microscope (SEM) Analysis

Scan Electron Microscope is useful in identifying the corrosion activities of Carbon Steel. Results from STEM often indicate the extent and nature of corrosion taking place at a particular time. The SEM analysis was conducted at pH 4.0 and pH 8.0. This result was also compared with the blank sample (without inhibitor concentration)

DOI: 10.31695/IJASRE.2020.33939

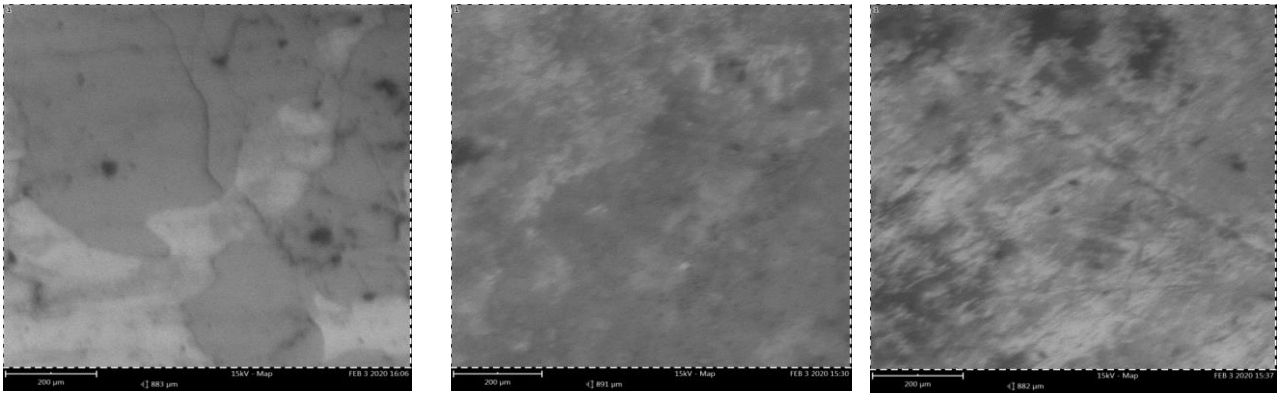

A B C

Fig3.10: (A) SEM analysis without the Inhibitor additive, (B) with the Inhibitor additive at pH 3.15 and (C) with the Inhibitor additive at pH 8.0

Observation of figure 3.10 (A) shows that there were patches of corrosion observed on the Carbon Steel and this was due to the dissolution of the Iron carbonate since there was no presence of an Inhibitor on the Carbon Steel (Abbasov, et al., 2013).

Figure 3.10 (B) and (C) shows the morphology of the Carbon Steel with the presence of the Inhibitor additive. It can be observed that the surface has a smooth appearance which is in agreement to the fact that corrosion was minimal on the surface of the Coupon. The reason for the smooth morphology observed was due to the Inhibitor occupying active sites needed for corrosion to take place. In addition, there was an attractive force between the Inhibitor molecules and the Metal surface (Singh, et al., 2013).

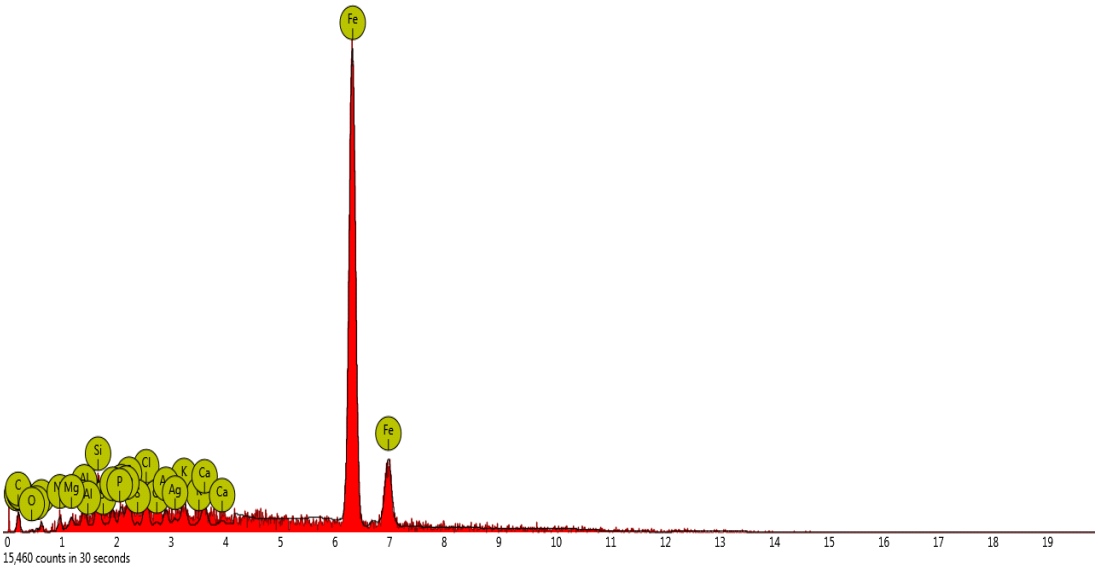

Figure 3.11: Scanning Electron Microscope of Carbon Steel at 200ppm pH 8

DOI: 10.31695/IJASRE.2020.33939

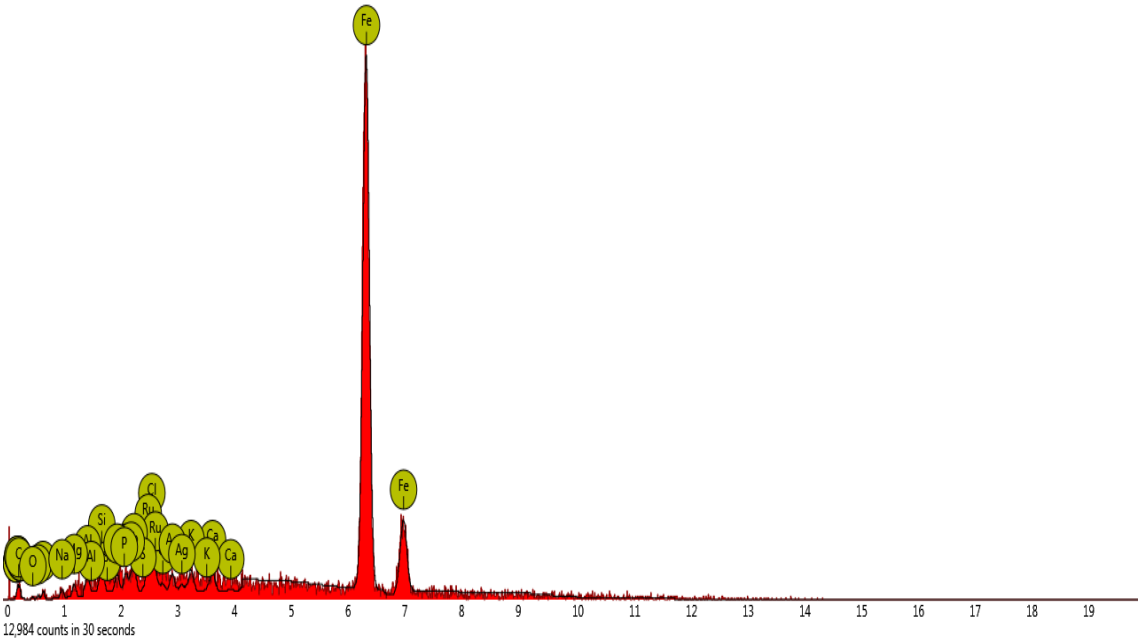

Figure 3.12: Scanning Electron Microscope of Carbon Steel at 200ppm pH 8

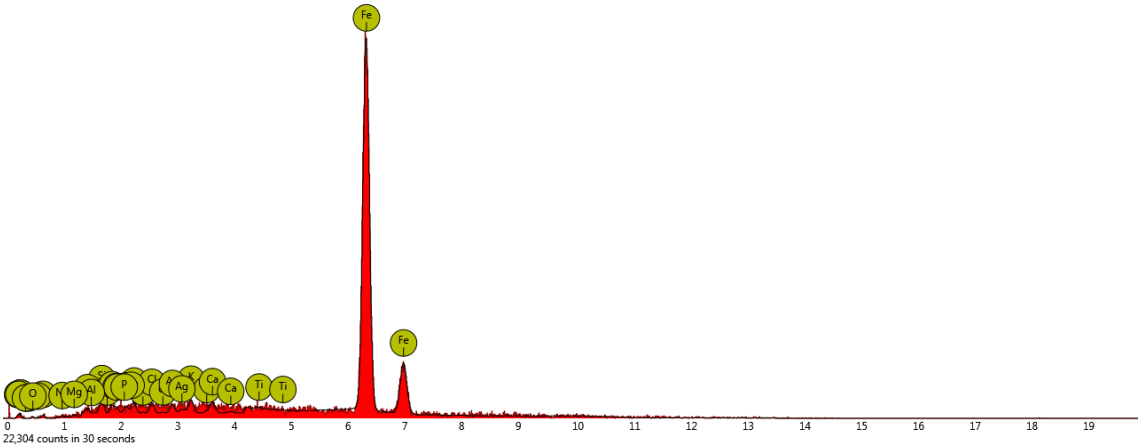

Figure 3.13: Scanning Electron Microscope of Carbon Steel for Blank

3.4 Gas Chromatography Mass Spectroscopy (GC-MS) Analysis

The GC-MS contains a Library of standard spectrum which was used to compare each of the chromatogram from the Carbon Steel Coupon that was used. From the Results (Figure 4.1-4.5) below, various similarities set result was obtained for each compound (Benedict, 2014).

DOI: 10.31695/IJASRE.2020.33939

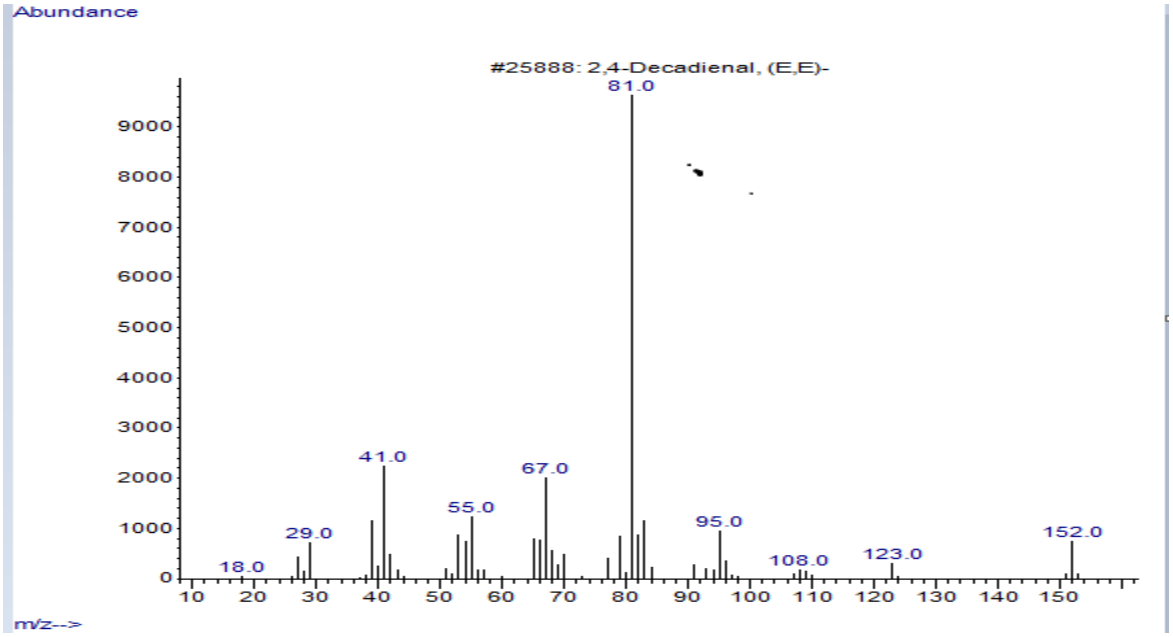

Figure 3.16: Gas Chromatography Mass Spectrometry analysis for 2,4-De cadienal

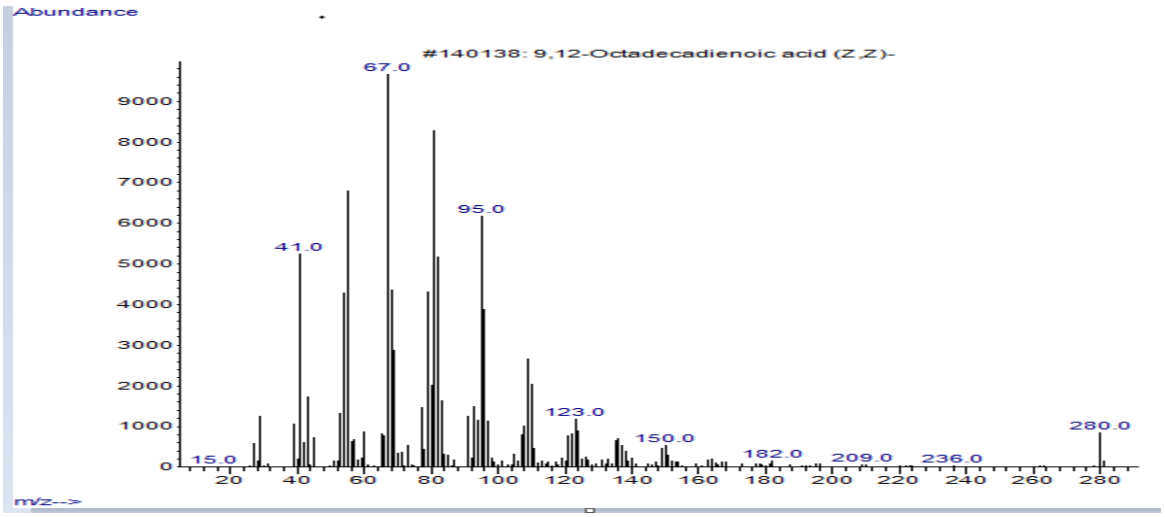

Figure 3.17: Gas Chromatography Mass Spectrometry analysis for 9,12-OctaDecadienoic acid

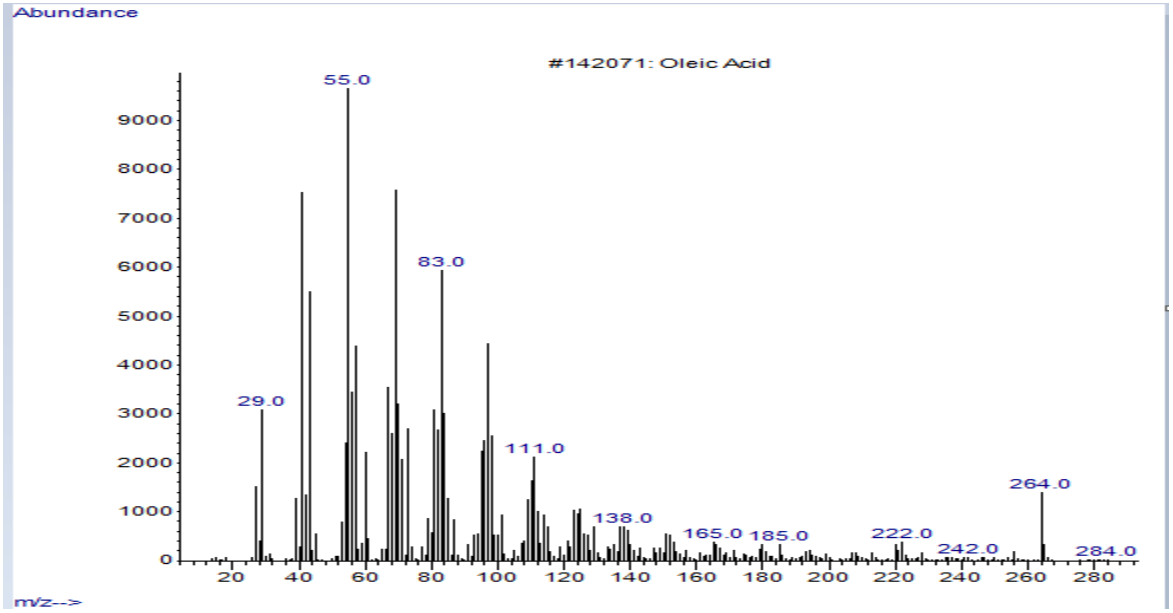

DOI: 10.31695/IJASRE.2020.33939

Figure 3.18: Gas Chromatography Mass Spectrometry analysis for Oleic acid

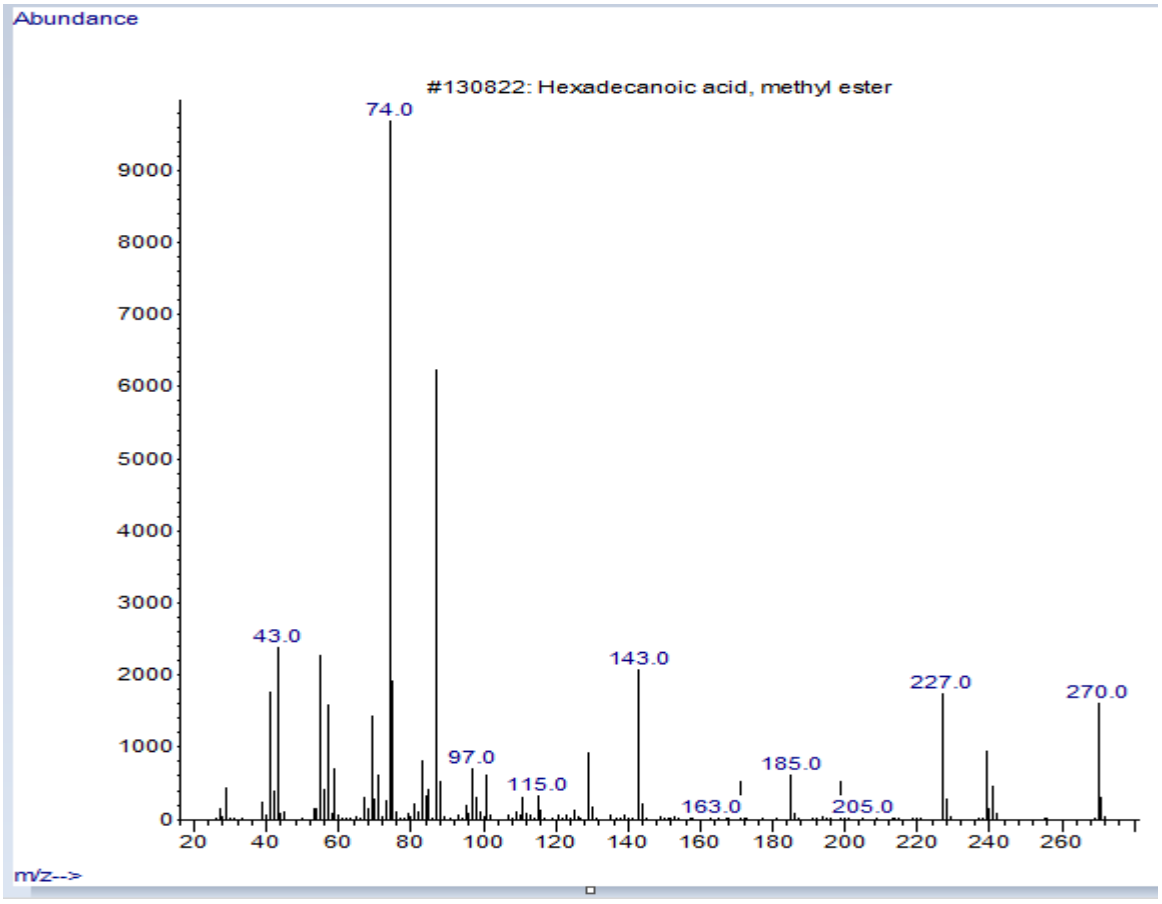

Figure 3.19: Gas Chromatography Mass Spectrometry analysis for Hexadecanoic Acid Methyl Ester

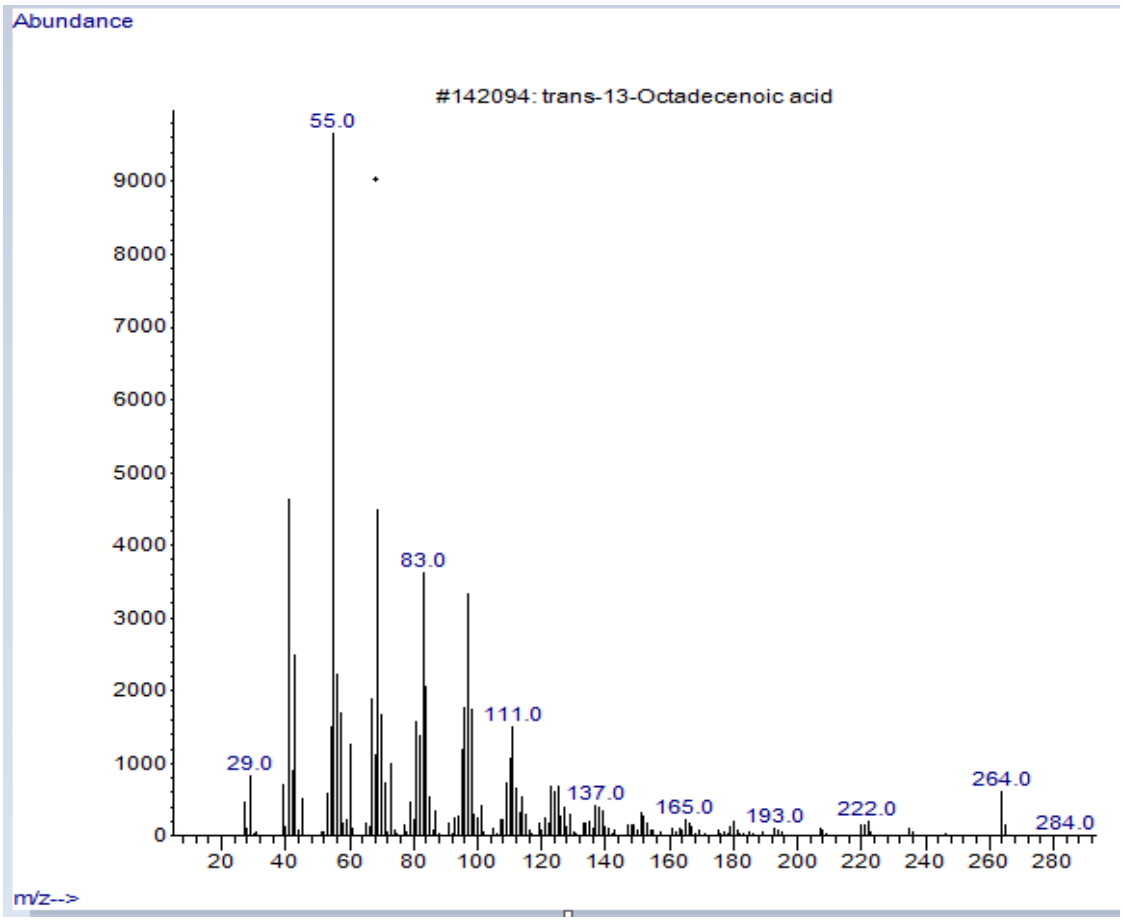

DOI: 10.31695/IJASRE.2020.33939

Figure 3.20: Gas Chromatography Mass Spectrometry analysis for Trans 13 Octadecanoic Acid

Figures 3.16-3.20 represents the characterisation of the Watermelon seed extract using GC-MS. Analysis of the results display the property that the Watermelon seed oil is made of. From the result, the Watermelon seed extract is made up of Oleic Acid, Decadieonic Acid, Hexadecanoic Acid etc These Compounds are capable of providing a strong bonding force needed on a Metal surface which can further help to slow down the rate of corrosion (Durowaye, et al., 2014).

4. CONCLUSION

The following conclusions were summarised from this study;

- The scanning Electron Microscope analysis on the A36 Carbon Steel revealed patches of corrosion at pH 3.15(Saturated solution) in the absence of Inhibitor concentration and a fewer patches at pH 8.0 with Inhibitor Concentration of 200mg/l. A smoother surface appearance was observed at pH 3.15 with same Inhibitor concentration at 24hrs time interval which indicated that the Citrillus lanatus is an active green Inhibitor on the Carbon Steel.
- As Inhibitor concentration increases, weight loss decreases, Corrosion rate decreaes while the Inhibitor Efficiency decreaes at the same pH level.
- As the exposure time increases, the difference in weight loss between each time interval reduces.
- The weight loss decrease with an increase in pH from 3.15 to 8.0.
- The GC-MS characterization of the Citrillus lanatus Extract showed that it is made up of constituents (Carboxylic Acid, Alkanal, Amide etc) that have hetero-atoms (NOS) in that is typical of good Corrosion Inhibitors.
- The Langmuir Adsorption isotherm accurately fitted the adsorption process of the Citrillus lanatus Extract on the surface of the A36 Carbon Steel with a slope (1.03) close to unity from the Langmuir Adsorption plot which was an indication that the Inhibitor occupies individual active sites of the Carbon Steel Coupon. Therefore, the adsorption process can be described as physisorption.
-

REFERENCES

1. Abbasov,V.M, Hany, M. Abd El-Lateef, L. I. Aliyeva, I. T. Ismayilov and Qasimov, E. E. 2013 *J. Korean Chem. Soc.*, , **57**, no. 1, 25.
2. Al-Haj-Ali, A.M., Jarrah, N.A., Mu'Azu, N.D., Rihan, R.O., 2014. Thermodynamics and kinetics of inhibition of aluminum in hydrochloric acid by date palm leaf extract. J. Appl. Sci. Environ. Manag. 18, 543–551.
3. Anbarai, C., Rajendran, S., Pandiarajan, M., and Krishnaveni,A ., 2013, An Encounter with Corrosion Inhibitors, European Chemical Bulletin, vol. 2, no. 4, pp. 197-207.
4. Aribo, S., Olusegun, S.J., Ibhadiyi, L.J., Oyetunji, A., Folorunso, D.O., 2017. Green inhibitors for corrosion Protection in acidizing oilfield environment. J. Assoc. Arab Univ. Basic Appl. Sci. 24, 34–38. https://doi.org/10.1016/j.jaubas.2016.08.001
5. Asadi, V., Danaee, I., Eskandari, H., 2015. The Effect of Immersion Time and Immersion Temperature on the Corrosion Behavior of Zinc Phosphate Conversion Coatings on Carbon Steel. Mater. Res. 18, 706-713.https://doi.org/10.1590/1516-1439.343814
6. Cen, H., Chen, Z., Guo, X., 2019. N, S co-doped carbon dots as effective corrosion inhibitor for carbon steel in CO2-saturated 3.5% NaCl solution. J. Taiwan Inst. Chem. Eng. 99, 224–238.
7. Chakravarthy, M.P., Mohana, K.N., 2014. Adsorption and Corrosion Inhibition Characteristics of Some Nicotinamide Derivatives on Mild Steel in Hydrochloric Acid Solution. ISRN Corros. 2014, 1–13. https://doi.org/10.1155/2014/687276

DOI: 10.31695/IJASRE.2020.33939

8. Chaouiki, A., Chafiq, M., Lgaz, H., Al-Hadeethi, M.R., Ali, I.H., Masroor, S., Chung, I.-M., 2020. Green Corrosion Inhibition of Mild Steel by Hydrazone Derivatives in 1.0 M HCl. Coatings 10, 640.

9. Chesnokova, M.G., Shalaj, V.V., Kraus, Y.A., Cherkashina, N.V., Mironov, A.Y., 2016. Analysis of corrosion defects on oil pipeline surface using scanning electron microscopy and soil thionic and sulfate-reducing bacteria quantification. Procedia Eng. 152, 247–250.

10. Dehghani, A., Bahlakeh, G., Ramezanzadeh, B., Ramezanzadeh, M., 2019. A combined experimental and theoretical study of green corrosion inhibition of mild steel in HCl solution by aqueous Citrullus lanatus fruit (CLF) extract. J. Mol. Liq. 279, 603–624.

11. Durowaye, S.I., Alabi, A.G.F., Sekunowo, O.I., Bolasodun, B., Rufai, I.O., 2014. Effects of pH Variation on Corrosion of Mild Steel in Bore-hole Water using 1M Sodium Hydroxide Solution. Int. J. Eng. Technol. 4, 7.

12. El-Lateef, H.M.A., Aliyeva, L.I., Abbasov, V.M., Ismayilov, T.I., 2012. Corrosion inhibition of low carbon steel in CO2 -saturated solution using Anionic surfactant 17.

13. Espinoza Vázquez, A., López Reséndiz, L.A., Figueroa, I.A., Rodríguez Gómez, F.J., Figueroa, M., Ángeles Beltrán, D., Castro, M., Miralrio, A., 2020. Corrosion inhibition assessment on API 5L X70 steel by preussomerin G immersed in saline and saline acetic. J. Adhes. Sci. Technol. 1–27.

14. Farhadian, A., Rahimi, A., Safaei, N., Shaabani, A., Abdouss, M., Alavi, A., 2020. A theoretical and experimental study of castor oil-based inhibitor for corrosion inhibition of mild steel in acidic medium at elevated temperatures. Corros. Sci. 175, 108871.

15. Fayomi, O.S.I., Akande, I.G., Nsikak, U., 2019. An Overview of Corrosion Inhibition using Green and Drug Inhibitors. J. Phys. Conf. Ser. 1378, 022022. https://doi.org/10.1088/1742-6596/1378/2/022022

16. Gerengi, H.; Uygur, I.; Solomon, M.; Yildiz, M.; Goksu, H. **2016** Evaluation of the inhibitive effect of Diospyros kaki (Persimmon) leaves extract on St37 steel corrosion in acid medium. Sustain. Chem. Pharm., 4, 57–66.

17. Go, L.C., Holmes, W., Hernandez, R., 2019. Sweet corrosion inhibition on carbon steel using waste activated sludge extract, in: 2019 IEEE Green Technologies Conference (GreenTech). IEEE, pp. 1–4.

18. Hassan, K.H., Khadom, A.A., Kurshed, N.H., 2016. Citrus aurantium leaves extracts as a sustainable corrosion inhibitor of mild steel in sulfuric acid. South Afr. J. Chem. Eng. 22,1–5.

19. Hribšek, U., n.d. Introduction to corrosion 12.

20. Hu, K.; Zhuang, J.; Zheng, C.; Ma, Z.; Yan, L.; Gu, H.; Zeng, X.; Ding, J (201**6**). Effect of novel cytosine-l-alanine derivative based corrosion inhibitor on steel surface in acidic solution. J. Mol. Liq., 222, 109–117

21. Husaini, M., Usman, B., Ibrahim, M.B., 2018. Evaluation of corrosion behaviour of aluminum in different environment. Bayero J. Pure Appl. Sci. 11, 88–92.

22. Hynes, N.R.J., Selvaraj, R.M., Mohamed, T., Mukesh, A.M., Olfa, K., Nikolova, M.P., 2020. Aerva lanata flowers extract as green corrosion inhibitor of low-carbon steel in HCl solution: an in vitro study. Chem. Pap. 1–10.

DOI: 10.31695/IJASRE.2020.33939

23. John, S., Salam, A., Baby, A.M., Joseph, A., 2019. Corrosion inhibition of mild steel using chitosan/TiO2 nanocomposite coatings. Prog. Org. Coat. 129, 254–259.

24. Khan, G., Basirun, W.J., Kazi, S.N., Ahmed, P., Magaji, L., Ahmed, S.M., Khan, G.M., Rehman, M.A., Badry, A.B.B.M., 2017. Electrochemical investigation on the corrosion inhibition of mild steel by Quinazoline Schiff base compounds in hydrochloric acid solution. J. Colloid Interface Sci. 502, 134–145.

25. Kina, A.Y. and Ponciano, J.A.C.(2013). Inhibition of Carbon Steel CO2 Corrosion in high salinity solutions. Int. J. Electrochem Sci. 8, 12600-12612

25. Kumar, K.P.V.; Pillai, M.S.N.; Thusnavis, G.R. 2011 Seed Extract of Psidiumguajava as Ecofriendly Corrosion Inhibitor for Carbon Steel in Hydrochloric Acid Medium.J. Mater. Sci. Technol., 27, 1143–1149.

26. Loto, R.T., 2018. Surface coverage and corrosion inhibition effect of Rosmarinus officinalis and zinc oxide on the electrochemical performance of low carbon steel in dilute acid solutions. Results Phys. 8, 172–179. https://doi.org/10.1016/j.rinp.2017.12.003

27. Lyon, S.; Bingham, R.; Mills, D. 2017 Corrosion Protection of Carbon Steel by Pongamiaglabra Oil- Based Polyetheramide Coatings.Prog. Org. Coat., 102, 2–7.

28. Mohammed, A.A., Manalo, A.C., Ferdous, W., Zhuge, Y., Vijay, P.V., Pettigrew, J., 2020. Experimental and numerical evaluations on the behaviour of structures repaired using prefabricated FRP composites jacket. Eng. Struct. 210, 110358.

29. Muthukrishnan, P.; Prakash, P.; Jeyaprabha, B.; Shankar, K. 2019. Stigmasterol extracted from Ficushispida leaves as a green inhibitor for the mild steel corrosion in 1 M HCl solution. Arab. J. Chem., 12, 3345–3356.

30. Nam, N.D., Bui, Q.V., Mathesh, M., Tan, M.Y.J., Forsyth, M., 2013. A study of 4-carboxyphenylboronic acid as a corrosion inhibitor for steel in carbon dioxide containing environments. Corros. Sci. 76, 257–266.

31. Obot, I.B., Onyeachu, I.B., Umoren, S.A., 2019. Alternative corrosion inhibitor formulation for carbon steel in CO2-saturated brine solution under high turbulent flow condition for use in oil and gas transportation pipelines. Corros. Sci. 159, 108140.

32. Odewunmi, N.; Umoren, S.; Gasem, Z.; Ganiyu, S.; Muhammad, Q. 2015 Electrochemical and quantum chemical studies on carbon steel corrosion protection in 1MH2SO4 using new eco-friendly Schi_ base metal complexes.J. Taiwan Inst. Chem. Eng., 51, 177–185.

33. Oloruntoba, D.T., Adesina, O.S., Falana, O., Akinluwade, K.J., 2020. Effect of Preheat Treatment on Wear and Corrosion Rates of Copper Electrodeposition on Medium-Carbon Steel. J. Fail. Anal. Prev. 20, 1754–1764.

34. Onyeachu, I.B., Obot, I.B., Adesina, A.Y., 2020. Green corrosion inhibitor for oilfield application II: The time evolution effect on the sweet corrosion of API X60 steel in synthetic brine and the inhibition performance of 2-(2-pyridyl) benzimidazole under turbulent hydrodynamics. Corros. Sci. 108589.

35. Palumbo, G., Górny, M., Banaś, J., 2019. Corrosion Inhibition of Pipeline Carbon Steel (N80) in CO2-Saturated Chloride (0.5 M of KCl) Solution Using Gum Arabic as a Possible Environmentally Friendly Corrosion Inhibitor for Shale Gas Industry. J. Mater. Eng. Perform. 28, 6458–6470. https://doi.org/10.1007/s11665-019-04379-3

DOI: 10.31695/IJASRE.2020.33939

36. Peng, S. and Zeng, Z. 2015 "An experimental study on the internal corrosion of a subsea multiphase pipeline"

, *Petroleum*, vol. 1, no. 1, pp. 75-81.

37. Qian, L.I., Sha-lin, Z., Zhen-bo, L.V., 2009. SYNERGISTIC INHIBITION EFFECT OF IMIDAZOLINE QUATEMARY-AMMONIUM-SALT AND ALKYL-PHOSPHATE ESTER IN A CO2-SATURATED ARTIFICIAL BRINE. Corros. Sci. Protetion Technol. 21, 571–573.

38. Ramezanzadeh, M., Bahlakeh, G., Sanaei, Z., Ramezanzadeh, B., 2019. Corrosion inhibition of mild steel in 1 M HCl solution by ethanolic extract of eco-friendly Mangifera indica (mango) leaves: electrochemical, molecular dynamics, Monte Carlo and ab initio study. Appl. Surf. Sci. 463, 1058–1077.

39. Rivera-Grau, L.M., Casales, M., Regla, I., Ortega-Toledo, D., Cuervo, D., Asencio, J., Gonzalez-Rodriguez, J., M Martine-Gomez, L., 2012. Corrosion inhibition by a coconut oil modified imidazoline for carbon steel under the combined effect of CO 2 and H 2 S. Int J Electrochem Sci 7, 12610–12620.

40. Salman, T.; Al-Azawi, K.; Mohammed, I.; Al-Baghdadi, S.; Al-Amiery, A.; Gaaz, T. 2018 Experimental and quantum chemical simulations on the corrosion inhibition of mild steel by 3-((5-(3,5-dinitrophenyl)-1,3,4-thiadiazol-2-yl)imino)indolin-2-one. Results Phys., 10, 291–296.

41. Singh, A., Ansari, K.R., Haque, J., Dohare, P., Lgaz, H., Salghi, R., Quraishi, M.A., 2018. Effect of electron donating functional groups on corrosion inhibition of mild steel in hydrochloric acid: Experimental and quantum

chemical study. J. Taiwan Inst. Chem. Eng. 82, 233–251.

42. Taheri, M., Naderi, R., Saremi, M., Mahdavian, M., 2017. Development of an ecofriendly silane sol-gel coating with zinc acetylacetonate corrosion inhibitor for active protection of mild steel in sodium chloride solution. J. Sol-Gel Sci. Technol. 81, 154–166.

43. Tariq Saeed, M., Saleem, M., Niyazi, A.H., Al-Shamrani, F.A., Jazzar, N.A., Ali, M., 2020. Carrot (Daucus Carota L.) Peels Extract as an Herbal Corrosion Inhibitor for Mild Steel in 1M HCl Solution. Mod. Appl. Sci. 14, 97.

https://doi.org/10.5539/mas.v14n2p97.

44. Tasić, Ž.Z., Mihajlović, M.B.P., Radovanović, M.B., Simonović, A.T., Antonijević, M.M., 2018. Cephradine as corrosion inhibitor for copper in 0.9% NaCl solution. J. Mol. Struct. 1159, 46–54.

45. Uddin, I., Khan, M.A., Ullah, S., Islam, S., Israr, M., Hussain, F., 2018. Characteristics of buoyancy force on stagnation point flow with magneto-nanoparticles and zero mass flux condition. Results Phys. 8, 160–168. https://doi.org/10.1016/j.rinp.2017.10.038

46. Verma, C., Ebenso, E.E., Quraishi, M.A., 2017. Corrosion inhibitors for ferrous and non-ferrous metals and alloys in ionic sodium chloride solutions: A review. J. Mol. Liq. 248, 927–942.

47. Yabuki, A.; Tanabe, S.; Fathona, I. 2018, Comparative studies of two benzaldehydethiosemicarbazone derivatives as corrosion inhibitors for mild steel in 1.0 M HCl. Surf. Coat. Technol. 341, 71–77.

48. Yao, J., Ge, H., Zhang, Y., Wang, X., Xie, S., Sheng, K., Meng, X. and Zhao, Y. (2020). Influence of Ph on corrosion inhibition of Carbon Steel in simulated cooling water containing scale and corrosion Inhibitors. Materials and Corrosion, 71(8).Pp 110-114

DOI: 10.31695/IJASRE.2020.33939

49. Zhang, J.; Qiao, G.; Hu, S.; Yan, Y.; Ren, Z.; Yu, L. 2011. Theoretical evaluation of corrosion inhibition performance of imidazoline compounds with di_erent hydrophilic groups. Corros. Sci., 53, 147–152

DOI: 10.31695/IJASRE.2020.33939